Pergamon

Int. J. Solids Structures Vol. 31, No. 4, pp. 533–550, 1994

0020–7683/94 $6.00 + .00

SHAPE OPTIMIZATION IN ELASTICITY AND ELASTO–VISCOPLASTICITY BY THE BOUNDARY ELEMENT METHOD

XIN WEI and ABHIJIT CHANDRA
Department of Aerospace and Mechanical Engineering, The University of Arizona, Tucson, AZ 85721, U.S.A.

LIANG-JENQ LEU and SUBRATA MUKHERJEE
Department of Theoretical and Applied Mechanics, College of Engineering, 212 Kimball Hall, Cornell University, Ithaca, NY 14853, U.S.A.

(*Received* 12 *December* 1992; *in revised form* 13 *August* 1993)

Abstract—This paper is concerned with the optimal shape design of solids undergoing small-strain, small-rotation, elasto–viscoplastic deformation. Shape sensitivities for this class of problems are determined by using a direct differentiation approach (DDA) to the governing boundary element method (BEM) equations of the problem. The standard BEM and the sensitivity equations are discretized and solved numerically. Shape optimization is carried out by coupling the standard and sensitivity analyses with an optimizer. The optimization algorithm chosen here uses sequential quadratic programming to obtain the desired optimal shape of a body in an iterative manner. Numerical solutions for optimal shapes of cutouts in plates (two-dimensional plane stress) are presented. The difference between optimal shapes of solids undergoing purely elastic and elasto–viscoplastic deformation is shown clearly in these examples.

1. INTRODUCTION

The optimal shape design of solid bodies undergoing small-strain elasto–viscoplastic deformation is investigated in this paper. The goal here is to maximize or minimize an objective function without violating certain constraints. The objective functions and constraints are typically functions of stresses and/or displacements, which, in turn, depend upon the initial shape of a body. The stresses and displacements in elasto–viscoplastic problems are time-dependent and also depend on the history of the deformation process. In this work, the design variables are taken to be shape parameters that define the initial shape of part or all of a body, and the objective function and constraint values are defined at a fixed time T from the start of the deformation process.

An optimization process starts with a preliminary design (first guess of the initial shape of the body). An elasto–viscoplastic analysis is carried out up to a fixed time T. Next, a sensitivity analysis is carried out up to the same time T, and the values of the design sensitivity coefficient (DSCs) are obtained at this time. This information (at time T) is input to an optimizer. Typically, an optimizer uses nonlinear programming to propose a new design (improved initial shape of the body) by providing a better value of the objective function without violating the constraints of a problem. If the new design is acceptable, the process stops. Otherwise, the interative process is continued, producing a succession of designs, until an optimal design (optimal initial shape of the body) is obtained.

In addition to successive simulations of an elasto–viscoplastic deformation process, the work described here has two additional important ingredients. The first is the accurate calculation of DSCs, which is discussed below. The second is the optimizer. In this work, a computer subroutine, based on the work of Schittkowski (1986), has been used for this purpose. This work uses a sequential quadratic programming algorithm to carry out the optimization process. The reader is referred to books by Banichuk (1983), Haftka *et al.* (1990) and Zhao (1991) for full descriptions of the optimization of elastic structures.

Accurate calculation of DSCs is vital for the success of an optimization process. Design

sensitivity coefficients are the rates of change of response quantities, such as stress or displacement in a loaded body, with respect to design variables. There is a rich literature on the subject of calculation of DSCs for linear problems, such as linear elasticity. The book by Haug *et al.* (1986) gives an excellent summary of research in this area up to that time. Basically, three different approaches have been used—the finite difference approach (FDA), the adjoint structure approach (ASA), and the direct differentiation approach (DDA). Also, both the finite element method (FEM) and the boundary element method (BEM) have been used for these analyses by different researchers.

Design sensitivity coefficients for nonlinear solid mechanics problems are of primary concern to this work. Arora and his co-workers (Wu and Arora, 1987; Cardoso and Arora, 1988; Tsay and Arora, 1990; Tsay *et al.*, 1990), Choi and his co-workers (Choi and Santos, 1987; Santos and Choi, 1988; Park and Choi, 1990) and Tortorelli (1988, 1990) have attempted nonlinear sensitivity problems with the FEM. Mukherjee and Chandra (1989) presented a BEM formulation for shape sensitivities for small-strain elasto–viscoplastic problems, and Zhang *et al.* (1992a) recently carried out a numerical implementation for this class of problems. A BEM formulation for fully nonlinear problems with both material and geometric nonlinearities has been published by Mukherjee and Chandra (1991), and Zhang *et al.* (1992b) have recently published a numerical implementation for these problems.

This paper first reviews the calculation of DSCs, for small-strain, two-dimensional, elasto–viscoplastic problems. The equations for the DSCs are obtained by the DDA of the governing BEM equations of the problem. Some modifications have been made to the equations presented by Zhang *et al.* (1992a), and these are discussed here. As has been pointed out in previous papers, since nonelastic strain rates are typically strongly nonlinear and sensitive functions of stresses and DSCs are derivatives of history-dependent response variables, the numerical process must be extremely accurate in order for the optimization process to succeed. The BEM, however, is known to be very accurate if its numerical implementation is carried out with care. These issues are discussed further later in this paper.

The rest of this paper is concerned with shape optimization problems. Optimal shapes for cutouts in plates are used as numerical examples. Careful attention is paid to the best way of characterizing the geometry of a cutout and the choice of optimization functions and constraints. Elastic optimization problems are solved in order to check numerical results against known solutions. Finally, numerical results are presented for the design of the shape of a cutout in a plate undergoing elasto–viscoplastic deformation.

2. EQUATIONS FOR TWO-DIMENSIONAL ELASTO–VISCOPLASTICITY

2.1. *The DBEM formulation for plane strain*

Following Zhang *et al.* (1992a), the rate form of the DBEM (derivative BEM) formulation for two-dimensional elasto–viscoplasticity (or elasto–plasticity) in a simply connected domain is ($i, j, k = 1, 2$):

$$0 = \int_{\partial B} [U_{ij}(\mathbf{b}, P, Q)\dot{\tau}_i(\mathbf{b}, Q) - W_{ij}(\mathbf{b}, P, Q)\dot{\Delta}_i(\mathbf{b}, Q)]\, \mathrm{d}S(Q) + 2G\dot{\varepsilon}_{ik}^{(n)}(\mathbf{b}, P)$$

$$\times \int_{\partial B} U_{ij}(\mathbf{b}, P, Q)n_k(\mathbf{b}, Q)\, \mathrm{d}S(Q) + \int_B 2GU_{ij,k}(\mathbf{b}, P, q)[\dot{\varepsilon}_{ik}^{(n)}(\mathbf{b}, q) - \dot{\varepsilon}_{ik}^{(n)}(\mathbf{b}, P)]\, \mathrm{d}A(q). \quad (1)$$

A two-dimensional body, B, has the boundary ∂B in the x_1–x_2 plane, and u_i, $\Delta_i = \partial u_i/\partial s$, τ_i and $\varepsilon_{ij}^{(n)}$ are the components of the displacement, its tangential derivative (s is the curvilinear length coordinate measured around ∂B in the anticlockwise sense), traction and nonelastic strain, respectively. A superposed dot denotes a time derivative (pseudo-time derivative for elasto–plasticity), and $\mathbf{b}$ is a vector of design variables. The trace, $\varepsilon^{(n)}$, in three

dimensions, $\varepsilon_{11}^{(n)}+\varepsilon_{22}^{(n)}+\varepsilon_{33}^{(n)}$, is assumed to vanish, but can be restored if desired (Mukherjee and Chandra, 1987). Also, P (or p) and Q (or q) are source and field points, with capital letters denoting points on ∂B and lower case letters denoting points inside B, and n_k are components of the unit outward normal to ∂B at a point Q on it. This normal is allowed to jump across a corner. A comma denotes a derivative with respect to the coordinates of a field point. Finally, the kernels U_{ij} and W_{ij} are as given by Zhang *et al.* (1992a).

Equation (1) is a modified version of eqn (1) in Zhang *et al.* (1992a). Their version had the domain integral

$$\int_B 2GU_{ij,k}(\mathbf{b}, P, q)\dot{\varepsilon}_{ik}^{(n)}(\mathbf{b}, q)\,\mathrm{d}A(q),$$

which is $O(1/r)$ singular for two-dimensional problems. Using the addition–subtraction method, one can write the above integral as

$$\int_B 2GU_{ij,k}(\mathbf{b}, P, q)[\dot{\varepsilon}_{ik}^{(n)}(\mathbf{b}, q)-\dot{\varepsilon}_{ik}^{(n)}(\mathbf{b}, P)]\,\mathrm{d}A(q)+2G\dot{\varepsilon}_{ik}^{(n)}(\mathbf{b}, P)\int_B U_{ij,k}(\mathbf{b}, P, q)\,\mathrm{d}A(q).$$

The first term above is the last term in eqn (1) while the second, by applying Gauss' theorem, becomes the second term in eqn (1). The above regularization makes the domain integral in eqn (1) completely regular. This improves the accuracy of the numerical solutions of the mechanics problem. The sensitivity version of eqn (1) above [eqn (8) of this paper] also has regular domain integrals, while the corresponding equation in Zhang *et al.* (1992a) [their eqn (13)] has $O(1/r)$ singular domain integrals. Numerical results for sensitivities from eqn (13) of Zhang *et al.* (1992a) are not accurate enough for the optimization algorithm to succeed in some cases, while those from the regularized version [eqn (8) of this paper] are more accurate and lead to convergent optimal solutions for the (inelastic) numerical examples discussed later in this paper. Thus, regularization of the sensitivity equations [eqn (13) in Zhang *et al.* (1992a)] has proved to be crucial in the present work. Numerical results from the present and the old [Zhang *et al.* (1992a)] formulations, for a particular example, are discussed later in Section 4.6.1 of this paper.

It has been found useful to add the equation ($i = 1, 2$)

$$0 = \int_{\partial B} \dot{\Delta}_i\,\mathrm{d}S, \tag{2}$$

which reflects continuity of the velocity at a point on ∂B. The addition of this equation has substantially reduced the condition number of the stiffness matrix obtained by discretizing eqn (1)—from around 80,000 to around 900 in one example. Also, inclusion of eqn (2) improves the symmetry of the numerical solution in problems that are physically symmetric. It should also be noted that, for some problems with prescribed velocity on a portion ∂B_1 of ∂B, prescription of the tangential derivative of the velocity on ∂B_1 might lead to loss of information on the velocity itself. This may lead to loss of uniqueness of the solution obtained from this formulation. In such cases, this difficulty can be overcome by appending constraint equations of the type

$$\dot{u}_i(B)-\dot{u}_i(A) = \int_A^B \dot{\Delta}_1\,\mathrm{d}S, \tag{3}$$

where A and B are suitably chosen points on the boundary ∂B.

As can be seen from eqn (1), the rates of traction and displacement derivative vectors

are the primary unknowns on ∂B. It can be shown that the rates of stress components at a regular point P on ∂B can be written in terms of the rates of the components of τ, Δ and ε^n as [see Sladek and Sladek (1986) and Cruse and Vanburen (1971) for the elastic case] (i, j, k, $l = 1, 2$)

$$\dot{\sigma}_{ij} = A_{ijk}\dot{\tau}_k + B_{ijk}\dot{\Delta}_k + C_{ijkl}\dot{\varepsilon}^{(n)}_{kl} + D_{ij}\dot{\varepsilon}^{(n)}_{kk}, \tag{4}$$

where A_{ijk}, etc., are functions of the components of the unit outward normal ($\mathbf{n}$) and unit (anticlockwise) tangent ($\mathbf{t}$) vectors to ∂B at P, and the shear modulus and Poisson's ratio G and ν, respectively, of the body. Explicit expressions for A_{ijk}, etc., are given by Zhang *et al.* (1992a) and are not repeated here.

The nonelastic problem also requires that strain and stress rates be obtained at internal points as functions of time. The form used here, in which the domain integrand is $Q(1/r)$ singular, is [$i, j, k, I = 1, 2$; $I = \partial/\partial x_I(p)$]

$$\dot{u}_{j,I}(\mathbf{b}, p) = \int_{\partial B} [U_{ij,I}(\mathbf{b}, p, Q)\dot{\tau}_i(\mathbf{b}, Q) - W_{ij,I}(\mathbf{b}, p, Q)\dot{\Delta}_i(\mathbf{b}, Q)]\, \mathrm{d}S(Q)$$

$$-2G\dot{\varepsilon}^{(n)}_{ik}(\mathbf{b}, p)\int_{\partial B} U_{ij,k}(\mathbf{b}, p, Q)n_l(\mathbf{b}, Q)\, \mathrm{d}S(Q)$$

$$+\int_B 2GU_{ij,kl}(\mathbf{b}, p, q)[\dot{\varepsilon}^{(n)}_{ik}(\mathbf{b}, q) - \dot{\varepsilon}^{(n)}_{ik}(\mathbf{b}, p)]\, \mathrm{d}A(q). \tag{5}$$

Finally, the stress rate components at an internal point are obtained from Hooke's law as ($i, j, k = 1, 2$)

$$\dot{\sigma}_{ij} = \lambda\dot{u}_{k,k}\delta_{ij} + G(\dot{u}_{i,j} + \dot{u}_{j,i}) - 2G\dot{\varepsilon}^{(n)}_{ij}, \tag{6}$$

where $\lambda = 2G\nu/(1-\nu)$ is the first Lamé constant. The formulation for plane stress is quite analogous to that described by Zhang *et al.* (1992a) and is not described here in the interest of brevity.

2.2. *Modeling of corners*

The modeling of corners on ∂B, using conforming boundary elements for elasticity problems, has been discussed in detail by Zhang and Mukherjee (1991), and the elasto–viscoplasticity case by Zhang *et al.* (1992a). Eight primary scalar quantities, τ_i^-, Δ_i^-, τ_i^+, and Δ_i^+ ($i = 1, 2$; $-$ denotes before and $+$ after a corner in a counterclockwise sense), are of interest at a corner. Four of these are prescribed from boundary conditions and two DBEM equations are available at a source point at a corner. If the stress components are continuous at a corner, one can write the following three additional scalar equations for plane strain ($i, j, k, l = 1, 2$)

$$A^-_{ijk}\dot{\tau}^-_k + B^-_{ijk}\dot{\Delta}^-_k + C^-_{ijkl}\dot{\varepsilon}^{(n)}_{kl} + D^-_{ij}\dot{\varepsilon}^{(n)}_{kk} = A^+_{ijk}\dot{\tau}^+_k + B^+_{ijk}\dot{\Delta}^+_k + C^+_{ijkl}\dot{\varepsilon}^{(n)}_{kl} + D^+_{ij}\dot{\varepsilon}^{(n)}_{kk}. \tag{7}$$

With $\dot{\varepsilon}^{(n)}_{ij}$ known at any time from a viscoplastic constitutive model (a discussion of such models appears later in this paper), the global system of equations is overdetermined because of one extra equation at each corner [from eqn (7) above]. The system, however, is consistent, has full rank, and the number of linearly independent equations equals the number of unknowns. Regular QR decomposition [see, for example, Golub and Van Loan (1989)] is used to solve this system of equations. The general situation for discontinuous σ across a corner for the linear elastic case is discussed in detail by Zhang and Mukherjee (1991).

3. SENSITIVITY EQUATIONS FOR PLANE STRAIN

The first step here is the differentiation of eqn (1) with respect to a design variable b (which is any component of the design vector $\mathbf{b}$). Let a superscribed asterisk (*) denote the design derivative (with respect to b) of a variable of interest and a superscribed circle (°) denote the design derivative of its rate [i.e. $\dot{\sigma}_{ij}^{*} = (\mathrm{d}/\mathrm{d}b)\sigma_{ij}$ and $\mathring{\sigma}_{ij} = (\mathrm{d}/\mathrm{d}b)\dot{\sigma}_{ij}$]. Now, one obtains the equations ($i, j, k = 1, 2$)

$$
\begin{aligned}
0 = & \int_{\partial B} [U_{ij}(\mathbf{b}, P, Q)\mathring{\tau}_i(\mathbf{b}, Q) - W_{ij}(\mathbf{b}, P, Q)\mathring{\Delta}_i(\mathbf{b}, Q)]\, \mathrm{d}S(Q) \\
& + \int_{\partial B} [\overset{*}{U}_{ij}(\mathbf{b}, P, Q)\dot{\tau}_i(\mathbf{b}, Q) - \overset{*}{W}_{ij}(\mathbf{b}, P, Q)\dot{\Delta}_i(\mathbf{b}, Q)]\, \mathrm{d}S(Q) \\
& + \int_{\partial B} [U_{ij}(\mathbf{b}, P, Q)\dot{\tau}_i(\mathbf{b}, Q) - W_{ij}(\mathbf{b}, P, Q)\dot{\Delta}_i(\mathbf{b}, Q)]\, \mathrm{d}\overset{*}{S}(Q) \\
& + 2G\mathring{\varepsilon}_{ik}^{(n)}(\mathbf{b}, P) \int_{\partial B} U_{ij}(\mathbf{b}, P, Q)n_k(\mathbf{b}, Q)\, \mathrm{d}S(Q) \\
& + 2G\dot{\varepsilon}_{ik}^{(n)}(\mathbf{b}, P) \int_{\partial B} \overset{*}{U}_{ij}(\mathbf{b}, P, Q)n_k(\mathbf{b}, Q)\, \mathrm{d}S(Q) \\
& + 2G\dot{\varepsilon}_{ik}^{(n)}(\mathbf{b}, P) \int_{\partial B} U_{ij}(\mathbf{b}, P, Q)\overset{*}{n}_k(\mathbf{b}, Q)\, \mathrm{d}S(Q) \\
& + 2G\dot{\varepsilon}_{ik}^{(n)}(\mathbf{b}, P) \int_{\partial B} U_{ij}(\mathbf{b}, P, Q)n_k(\mathbf{b}, Q)\, \mathrm{d}\overset{*}{S}(Q) \\
& + \int_{B} 2G\overset{*}{U}_{ij,k}(\mathbf{b}, P\, q)[\dot{\varepsilon}_{ik}^{(n)}(\mathbf{b}, q) - \dot{\varepsilon}_{ik}^{(n)}(\mathbf{b}, P)]\, \mathrm{d}A(q) \\
& + \int_{B} 2GU_{ij,k}(\mathbf{b}, P, q)[\mathring{\varepsilon}_{ik}^{(n)}(\mathbf{b}, q) - \mathring{\varepsilon}_{ik}^{(n)}(\mathbf{b}, P)]\, \mathrm{d}A(q) \\
& + \int_{B} 2GU_{ij,k}(\mathbf{b}, P, q)[\dot{\varepsilon}_{ik}^{(n)}(\mathbf{b}, q) - \dot{\varepsilon}_{ik}^{(n)}(\mathbf{b}, P)]\, \mathrm{d}\overset{*}{A}(q),
\end{aligned} \tag{8}
$$

where, at the start of a time step, half the sensitivities of the rates of Δ_i and τ_i are to be determined and the rest of the quantities are known. The rates of τ_i, Δ_i and $\varepsilon_{ij}^{(n)}$ are known from the solution of the usual DBEM problem, up to this time, and the sensitivity of the nonelastic strain rate is known from differentiating a suitable constitutive model (Zhang *et al.*, 1992a). Formulae for $\overset{*}{U}_{ij}, \overset{*}{W}_{ij}, \overset{*}{U}_{ij,k}$ [i.e. $\mathrm{d}/\mathrm{d}b(U_{ij,k})$], $\mathrm{d}\overset{*}{S}$, $\mathrm{d}\overset{*}{A}$, n_k and $\overset{*}{n}_k$ are given by Zhang *et al.* (1992a).

Derivatives of eqns (2), (3) and (4) take the forms

$$
0 = \int_{\partial B} \mathring{\Delta}_i\, \mathrm{d}S + \int_{\partial B} \dot{\Delta}_i\, \mathrm{d}\overset{*}{S}, \tag{9}
$$

$$
\mathring{u}_i(B) - \mathring{u}_i(A) = \int_A^B \mathring{\Delta}_i\, \mathrm{d}S + \int_A^B \dot{\Delta}_i\, \mathrm{d}\overset{*}{S}, \tag{10}
$$

$$
\mathring{\sigma}_{ij} = A_{ijk}\mathring{\tau}_k + B_{ijk}\mathring{\Delta}_k + C_{ijkl}\mathring{\varepsilon}_{kl}^{(n)} + D_{ij}\mathring{\varepsilon}_{kk}^{(n)} + \dot{A}_{ijk}\dot{\tau}_k + \dot{B}_{ijk}\dot{\Delta}_k + \dot{C}_{ijkl}\dot{\varepsilon}_{kl}^{(n)} + \dot{D}_{ij}\dot{\varepsilon}_{kk}^{(n)}. \tag{11}
$$

Finally, one must derive an equation for the sensitivities of the velocity gradients at an internal point. The resulting equation has the form (all indices = 1, 2)

$$\begin{aligned}
\mathring{u}_{j,I}(\mathbf{b},p) = &\int_{\partial B} [U_{ij,I}(\mathbf{b},p,Q)\mathring{t}_i(\mathbf{b},Q) - W_{ij,I}(\mathbf{b},p,Q)\mathring{\Delta}_i(\mathbf{b},Q)]\,\mathrm{d}S(Q)\\
&+\int_{\partial B} [\dot{U}_{ij,I}(\mathbf{b},p,Q)\dot{t}_i(\mathbf{b},Q) - \dot{W}_{ij,I}(\mathbf{b},p,Q)\dot{\Delta}_i(\mathbf{b},Q)]\,\mathrm{d}S(Q)\\
&+\int_{\partial B} [U_{ij,I}(\mathbf{b},p,Q)\dot{\tau}_i(\mathbf{b},Q) - W_{ij,I}(\mathbf{b},p,Q)\dot{\Delta}_i(\mathbf{b},Q)]\,\mathrm{d}\dot{S}(Q)\\
&-2G\mathring{\varepsilon}^{(n)}_{ik}(\mathbf{b},p)\int_{\partial B} U_{ij,k}(\mathbf{b},p,Q)n_l(\mathbf{b},Q)\,\mathrm{d}S(Q)\\
&-2G\dot{\varepsilon}^{(n)}_{ik}(\mathbf{b},p)\int_{\partial B} \dot{U}_{ij,k}(\mathbf{b},p,Q)n_l(\mathbf{b},Q)\,\mathrm{d}S(Q)\\
&-2G\dot{\varepsilon}^{(n)}_{ik}(\mathbf{b},p)\int_{\partial B} U_{ij,k}(\mathbf{b},p,Q)\dot{n}_l(\mathbf{b},Q)\,\mathrm{d}S(Q)\\
&-2G\dot{\varepsilon}^{(n)}_{ik}(\mathbf{b},p)\int_{\partial B} U_{ij,k}(\mathbf{b},p,Q)n_l(\mathbf{b},Q)\,\mathrm{d}\dot{S}(Q)\\
&+\int_B 2GU_{ij,kI}(\mathbf{b},p,q)[\mathring{\varepsilon}^{(n)}_{ik}(\mathbf{b},q) - \mathring{\varepsilon}^{(n)}_{ik}(\mathbf{b},p)]\,\mathrm{d}A(q)\\
&+\int_B 2G\dot{U}_{ij,kI}(\mathbf{b},p,q)[\dot{\varepsilon}^{(n)}_{ik}(\mathbf{b},q) - \dot{\varepsilon}^{(n)}_{ik}(\mathbf{b},p)]\,\mathrm{d}A(q)\\
&+\int_B 2GU_{ij,kI}(\mathbf{b},p,q)[\dot{\varepsilon}^{(n)}_{ik}(\mathbf{b},q) - \dot{\varepsilon}^{(n)}_{ik}(\mathbf{b},p)]\,\mathrm{d}\dot{A}(q), \qquad (12)
\end{aligned}$$

where $\dot{U}_{ij,kI} = \mathrm{d}/\mathrm{d}b(U_{ij,kI})$.

The entire right-hand side of equation (12) is known at this stage, so that the required sensitivity of the velocity gradient at an internal point, $\mathring{u}_{j,I} = \mathrm{d}/\mathrm{d}b(\dot{u}_{j,I})$, can be obtained by a series of function evaluations. The boundary kernels are regular, and the domain integrands are $1/r$ singular. These singular integrals are numerically evaluated by the polar mapping method [Mukherjee (1982), see also, Nagarajan and Mukherjee (1993)].

Stress rate sensitivities at an internal point are obtained from a differential version of Hooke's law [eqn (6)]

$$\mathring{\sigma}_{ij} = \lambda\mathring{u}_{k,k}\delta_{ij} + G(\mathring{u}_{i,j} + \mathring{u}_{j,i}) - 2G\mathring{\varepsilon}^{(n)}_{ij}. \qquad (13)$$

The sensitivity equations at a corner, across which σ_{ij} and $\dot{\sigma}_{ij}$ are continuous, have the form

$$\mathring{\sigma}^{-}_{ij} = \mathring{\sigma}^{+}_{ij}, \qquad (14)$$

with $\mathring{\sigma}_{ij}$, at either side of a corner, given by eqn (11).

A discussion of the general form of viscoplastic constitutive equations and their sensitivities appears in Zhang *et al.* (1992a).

4. OPTIMIZATION OF PLATES WITH CUTOUTS

4.1. *Parameterization of cutout geometry*

The problem here concerns plates of arbitrary shape, in plane stress, with a traction-free cutout inside the plate. The plate material can be linear elastic or elasto–viscoplastic. With the global x_1 and x_2 axes centered at the center of a cutout, a variety of smooth curves

(e.g. a circle, an ellipse or a rectangle with rounded corners) can be represented by the equations (Sadegh, 1988; Lekhnitski, 1968)

$$x_1 = a(\cos\theta + \varepsilon\cos 3\theta), \tag{15}$$

$$x_2 = a(\beta\sin\theta - \varepsilon\sin 3\theta), \tag{16}$$

where a controls the size, ε the shape, and β the aspect ratio of the smooth cutout.

For example, with $\beta = 1$, a slight variation of the above equations is

$$x_1 = \frac{a}{1+\varepsilon}(\cos\theta + \varepsilon\cos 3\theta), \tag{17}$$

$$x_2 = \frac{a}{1+\varepsilon}(\sin\theta - \varepsilon\sin 3\theta), \tag{18}$$

where the points $(a, 0)$ (with $\theta = 0$) and $(0, a)$ (with $\theta = \pi/2$) are points on the curve. Considering a fixed and ε variable, $\varepsilon = -0.15$, for example, gives a square with rounded corners and $\varepsilon = 0$, of course, is a circle.

4.2. *Objective functions and constraints*

The optimization problem is set up as

$$\min \phi(b_i), \tag{19}$$

subject to the constraints

$$f_i(b_j) \geqslant 0. \tag{20}$$

Various choices are possible for the objective function ϕ. Two of these are

$$\phi_1 = \int_{\partial B_o} \tau_i u_i \, dS, \tag{21}$$

$$\phi_2 = \frac{1}{L}\int_{\partial B_c} (\sigma_{tt}(S) - \bar{\sigma}_{tt})^2 \, dS, \tag{22}$$

where ∂B_o is the outer boundary, ∂B_c is the cutout boundary, σ_{tt} is the tangential stress on the cutout boundary, $\bar{\sigma}_{tt}$ is the mean value of σ_{tt}, and L is the total length of the cutout boundary.

Equations (19) and (21) express the requirement of minimizing the external work done on the body (on a traction-free cutout, $\tau = 0$), and eqns (19) and (22) express the requirement of minimizing the variance of the tangential stress on the cutout, thereby requiring the tangential stress on the cutout to be as uniform as possible. *It is very important to note that, for time-dependent elasto–viscoplastic problems, an objective function is defined here as the value of ϕ at a fixed time T from the start of the deformation process.* The constraints used in these problems are related to bounds on the shape design variables.

4.3. *Numerical implementation and solution strategy*

Numerical implementation of the standard elasto–viscoplastic problem and the sensitivity problem follows the usual practice [see Zhang *et al.* (1992a)]. The boundary ∂B of the body is subdivided into piecewise quadratic, conforming boundary elements. The variables $\dot{\tau}_i$ and $\dot{\Delta}_i$ and their sensitivities are assumed to be piecewise quadratic on the boundary elements. The domain B of the body is divided into $Q4$ internal cells. The nonelastic strain rate components, $\dot{\varepsilon}_{ij}^{(n)}$, and their sensitivities, as well as the quantity $d\dot{A}/dA$, are interpolated on the $Q4$ internal cells.

Logarithmically singular integrands are integrated with log-weighted Gaussian integration formulae. The $O(1/r)$ singular domain integrals are regularized by polar coordinate mapping (Mukherjee, 1982) and then evaluated by Gaussian quadrature on a square. Typical numbers of Gauss points used are 20 and 16 for regular and log-singular boundary integrals and 3×3 for regular and regularized domain integrals.

The solution strategy for the standard and sensitivity problems, which involves solutions of appropriate equations at the start of each time step, together with marching forward in time, is described in some detail by Zhang *et al.* (1992a). Time integration has been carried out with fixed time steps. Optimal shape design is carried out by coupling the standard and sensitivity analyses with an optimizer (Schittkowski, 1986).

4.4. *The optimizer used in this work*

The subroutine N0ONF (available from the IMSL library) has been used to obtain optimal solutions in the present study. This subroutine is based on the subroutine NLPQL, a FORTRAN code developed by Schittkowski (1986). A brief description of the algorithm is given below. Further details are available in the above paper.

A typical nonlinear optimization problem is stated as follows:

$$\min \phi(\mathbf{b}), \quad \mathbf{b} \in R^n$$

$$\begin{aligned} \text{subject to } & h_j(\mathbf{b}) = 0, && \text{for } j = 1, \ldots, m, \\ & g_k(\mathbf{b}) \geqslant 0, && \text{for } k = 1, 2, \ldots, p, \\ & b_l \leqslant b_i \leqslant b_u, && \text{for each component } b_i \text{ of } \mathbf{b}, \end{aligned}$$

where $\phi(\mathbf{b})$ is the objective function, $\mathbf{b}$ is the design variable vector with n components, b_l and b_u are lower and upper bounds for each component of $\mathbf{b}$, and $h_j(\mathbf{b})$ and $g_k(\mathbf{b})$ are equality and inequality constraints, respectively.

The sequential quadratic programming algorithm NLPQL uses a quadratic approximation of the Lagrangian and linearization of the constraints to define a sequence of subproblems. This requires the evaluation of a positive definite approximation of the Hessian of ϕ.

Let $\mathbf{d}_k$ be the solution of a subproblem at the kth iterative step. A line search is used to find a new design, $\mathbf{b}_{k+1}$, defined as

$$\mathbf{b}_{k+1} = \mathbf{b}_k + \lambda_k \mathbf{d}_k, \qquad 0 < \lambda_k < 1 \quad (\text{no sum on } k),$$

such that the augmented Lagrangian function has a lower function value at the new design. Here, λ_k is the line search or step length parameter.

The iterative process stops when the Kuhn–Tucker optimality conditions are satisfied within an acceptable tolerance. Schittkowski (1986) shows that, under some mild assumptions, the algorithm converges globally, i.e. starting from an arbitrary initial point, at least one accumulation point of the iterates will satisfy the Kuhn–Tucker optimality conditions.

Coupling of the optimizer with the mechanics and sensitivity calculations is straightforward. One must input the functions ϕ, $\partial\phi/\partial b_i$, h_j, g_k, $\partial h_j/\partial b_i$ and $\partial g_k/\partial b_i$ at each iteration. Typically, ϕ, h_j and g_k depend on quantities such as stress or displacement and are, therefore, implicit as well as explicit functions of $\mathbf{b}$. The gradients of these functions, with respect to b_i, are obtained from the sensitivities, such as $\mathrm{d}\boldsymbol{\sigma}/\mathrm{d}\mathbf{b}$, by the chain rule of differentiation. It is important to note that, for elasto–viscoplastic problems, the above functions and their gradients are evaluated at a preset time T from the start of the simulation. This optimizer performs very well for the problems considered in this work, provided that the sensitivities are obtained with sufficient accuracy.

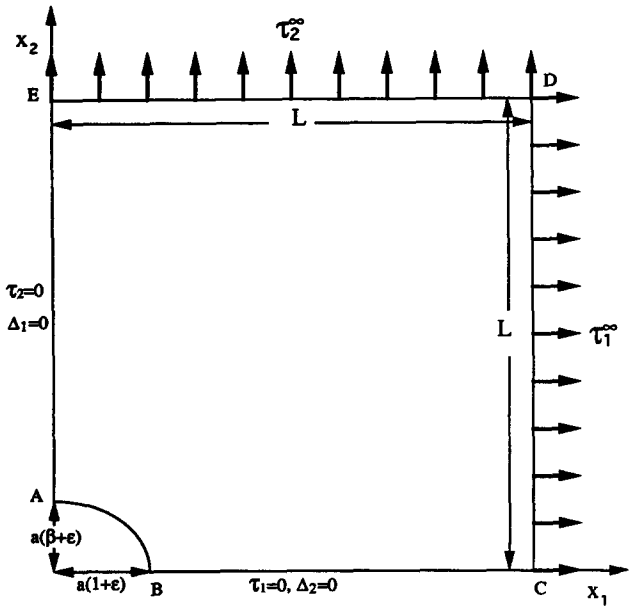

Fig. 1. Optimal shape design of a cutout in a plate.

4.5. *Elastic shape optimization*

These numerical examples have been solved in order to check the performance of the computer program against known elastic solutions.

(a) *Minimize external work.* In this case, the objective function is ϕ_1 from eqn (21) so that

$$\dot{\phi}_1 = \int_{\partial B_0} \dot{\bar{\tau}}_i u_i \, dS + \int_{\partial B_0} t_i \dot{u}_i \, dS + \int_{\partial B_0} \tau_i u_i \, d\dot{S}. \tag{23}$$

The plate is square, and the cutout shape is defined by eqns (15) and (16) with $\beta = 1$, a fixed, and ε the only design variable. Thus, the points $[a(1+\varepsilon), 0]$ and $[0, a(1+\varepsilon)]$ lie on the cutout. A quarter of the plate is modeled because of symmetry (Fig. 1 and Table 1). Uniform biaxial loading, $\tau_1^\infty = \tau_2^\infty = 1$ MPa, is applied to the plate. The constraints used in this problem are

$$-0.15 \leqslant \varepsilon \leqslant 0.10. \tag{24}$$

Table 1. Geometrical and loading parameters for various optimization problems for cutouts in plates

Problem	Parameters
Elastic problem (a)	$L = 30$ m $a = 2/(1+\varepsilon_0) = 2.353$ m $\beta = 1$ $\varepsilon \equiv$ design variable $\tau_1^\infty = \tau_2^\infty = 1$ MPa
Elastic problem (b)	$L = 5$ m $a = 1$ m $\varepsilon = 0$ $\beta \equiv$ design variable $\tau_1^\infty = 4$ MPa $\tau_2^\infty = 3$ MPa
Elastic–viscoplastic problem	$L = 5$ m $a = 1$ m $\varepsilon = 0$ $\beta \equiv$ design variable $\tau_1^\infty = S(t) = 8+4t$ MPa (t in seconds) $\tau_2^\infty = 0.75\, S(t)$, $T = 4$ s $\Delta t = 0.2$ s for $0 \leqslant t \leqslant 2$ s; 0.05 s for $2 \leqslant t \leqslant 4$ s

The expression for $\mathrm{d}\dot{S}/\mathrm{d}S$ on the cutout boundary AB can be easily obtained from eqns (17) and (18) and Zhang's *et al.*'s (1992a) eqn (17). The expressions for the normal $\mathbf{n}$ and $\dot{\mathbf{n}}$ on AB are obtained from Zhang *et al.*'s eqn (19). Using a linear approximation for the design velocities on the lines EA and BC, one gets:

$$\text{on } BC: \dot{x}_1 = \frac{a(L-x_1)}{L-a(1+\varepsilon)}, \quad \dot{x}_2 = 0, \quad \frac{\mathrm{d}\dot{S}}{\mathrm{d}S} = -\frac{a}{L-a(1+\varepsilon)}, \tag{25}$$

$$\text{on } AE: \dot{x}_1 = 0, \quad \dot{x}_2 = \frac{a(L-x_2)}{L-a(1+\varepsilon)}, \quad \frac{\mathrm{d}\dot{S}}{\mathrm{d}S} = -\frac{a}{L-a(1+\varepsilon)}. \tag{26}$$

Design velocities and $\mathrm{d}\dot{S}/\mathrm{d}S$ are zero on the lines CD and DE in Fig. 1.

The shape of the cutout, at different iterations, is shown in Fig. 2. The converged solution, after seven iterations, is $\varepsilon = -0.01515$. The well-known optimal analytical solution for a cutout in an infinite elastic plate (Banichuk, 1983) is a circle with $\varepsilon = 0$.

(b) *Minimize variance of tangential stress around cutout boundary.* In this case, the objective function is ϕ_2 from eqn (22) so that

$$\dot{\phi}_2 = -\frac{\dot{L}}{L}\phi_2 + \frac{1}{L}\int_A^B 2(\sigma_{tt}-\bar{\sigma}_{tt})(\dot{\sigma}_{tt}-\dot{\bar{\sigma}}_{tt})\,\mathrm{d}S + \frac{1}{L}\int_A^B (\sigma_{tt}-\bar{\sigma}_{tt})^2\,\mathrm{d}\dot{S}, \tag{27}$$

where

$$\dot{\bar{\sigma}}_{tt} = -\frac{\dot{L}}{L}\bar{\sigma}_{tt} + \frac{1}{L}\int_A^B \dot{\sigma}_{tt}\,\mathrm{d}S + \frac{1}{L}\int_A^B \sigma_{tt}\mathrm{d}\dot{S},$$

$$L = \int_A^B \mathrm{d}S \quad \text{and} \quad \dot{L} = \int_A^B \mathrm{d}\dot{S}.$$

The plate is square, as before. This time, an elliptical cutout boundary is modeled as

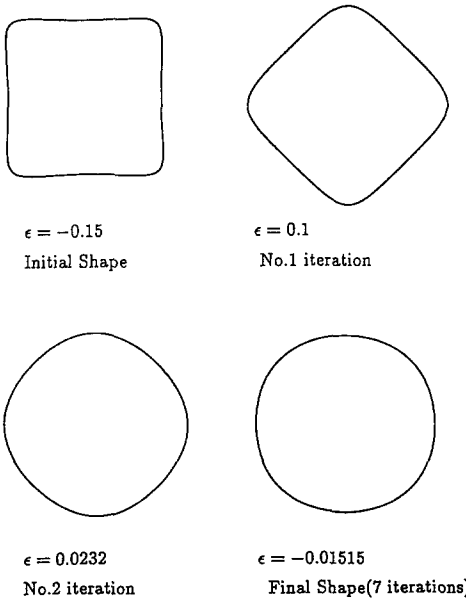

Fig. 2. Shapes of cutout at different iterations for the elastic optimization problem (a).

$$x_1 = a\cos\theta, \quad x_2 = b\sin\theta, \tag{28}$$

with a fixed and $b = a\beta$ the design variable. The constraint used in this problem is

$$0.3 \leqslant \beta \leqslant 1.0. \tag{29}$$

referring to Fig. 1 and Table 1, this time $a = 1.0$, $\varepsilon = 0$, $L = 5$ m, $\tau_1^\infty = S = 4$ MPa, and $\tau_2^\infty = (3/4)S = 3$ MPa.

Once again, the expression for $\mathrm{d}\hat{S}/\mathrm{d}S$ over the cutout boundary AB can be obtained easily. A linear approximation is used for the design velocity on the line EA. The design velocity is zero on the rest of the boundary BCDE. The actual formulae are given later.

The results for successive iterations are given in Table 2. The convergent solution is $\beta = 0.756$. It is well known (Banichuk, 1983) that the optimal analytical solution for a cutout in an infinite elastic plate, in this case, is an ellipse with $\beta = 0.75$.

4.6. *Elasto–viscoplastic shape optimization*

4.6.1. *Constitutive model and numerical issues.* The illustrative viscoplastic constitutive model used in this work is due to Anand (1982). The constitutive equations and material parameters used here are the same as those described by Zhang *et al.* (1992a).

As discussed before [e.g. Zhang *et al.* (1992a, b)], demands on numerical accuracy in these problems are quite stringent, especially for the calculation of the rates of sensitivities of stresses. It has proved very useful to check numerical results for benchmark problems against semi-analytical solutions.

Such a benchmark problem, that of a circular plate with a concentric circular cutout, subjected to spatially uniform external pressure that increases in time at a constant rate, is described in detail by Zhang *et al.* (1992a). A semi-analytical solution for this problem is also given in that paper. As discussed by Zhang *et al.*, semi-analytical solutions for sensitivities have been obtained both by analytical differentiation (ADD) and finite differencing (FDD) of direct solutions of the corresponding mechanics problem. These solutions agree within plotting accuracy (see Fig. 9 of Zhang *et al.*, 1992a). Since time integration can be fairly expensive, it appears best, at first, to suddenly apply a large pressure on the boundary of a disc and compare the BEM rates against semi-analytical ones. An example of such an exercise is given below. The problem chosen here is that of an annular circular disc, of inside and outside radii $a = 1.0$ m and $b = 1.5$ m, respectively, with a suddenly applied external pressure of 12 MPa. The inner radius is the design variable. The mesh and material model used are exactly the same as those for the corresponding problem by Zhang *et al.* (1992a). The results are shown in Table 3. It should be emphasized that, while the problem is axisymmetric, the BEM program is a general two-dimensional one.

In Table 3, an "analytical" solution is an exact solution for an elastic annular disc while a "semi-analytical" solution is obtained by numerical time integration of a system of differential equations governing the elasto–viscoplastic deformation of an axisymmetric hollow disc. These equations, in cylindrical coordinates, are given as eqns (30)–(33) in Zhang *et al.* (1992a). It should be noted here that the "semi-analytical" sensitivity equations

Table 2. Values of β and ϕ_2 at different iterations for the elastic shape optimization problem (b)†

Number of iterations	$\beta = b/a$	ϕ_2 (MPa^2)
1	1.000	2.70200
2	0.300	15.28900
3	0.814	0.17960
4	0.738	0.01720
5	0.756	0.00098

† CPU time = 29.78 s on an IBM 3090 supercomputer.

Table 3. Comparison of tangential stress σ_{tt},$\dot{\sigma}_{tt}$, $\dot{\sigma}_{tt}$ and $\mathring{\sigma}_{tt}$ around cutout in circular disk: BEM and analytical or semi-analytical solutions [see Zhang *et al.* (1992a)]

Location around circular cutout, θ (degrees)	Elastic				Elastic–viscoplastic			
	σ_{tt} (MPa)		$\dot{\sigma}_{tt}$ (MPa/m)		$\dot{\sigma}_{tt}$ (MPa s^{-1})		$\mathring{\sigma}_{tt}$ (MPa m^{-1} s^{-1})	
	BEM	Anal.	BEM	Anal.	BEM	Semi-anal.	BEM	Semi-anal.
0	−43.21	−43.2	−69.28	−69.12	207.77	205.01	2081.1	2072.7
9	−43.19	−43.2	−69.03	−69.12	204.39	205.01	2097.3	2072.7
18	−43.20	−43.2	−69.26	−69.12	204.97	205.01	2051.1	2072.7
27	−43.20	−43.2	−69.02	−69.12	202.14	205.01	2070.9	2072.7
36	−43.19	−43.2	−69.25	−69.12	203.15	205.01	2028.2	2072.7
45	−43.20	−43.2	−69.02	−69.12	201.38	205.01	2063.3	2072.7
54	−43.19	−43.2	−69.25	−69.12	203.16	205.01	2028.6	2072.7
63	−43.20	−43.2	−69.02	−69.12	202.15	205.01	2072.0	2072.7
72	−43.20	−43.2	−69.26	−69.12	204.99	205.01	2052.4	2072.7
81	−43.19	−43.2	−69.04	−69.12	204.41	205.01	2099.4	2072.7
90	−43.21	−43.2	−69.28	−69.12	207.80	205.01	2083.3	2072.7

are obtained by analytical differentiation of the mechanics equations. These "semi-analytical" solutions can be considered, for practical purposes, to be exact. Of course, they are used to benchmark the numerical DBEM solutions for special illustrative problems and are not available for general two-dimensional problems. Finally, "BEM" in Table 3 refers to numerical solutions from the present, general, two-dimensional DBEM approach.

The sensitivity history for a problem of pressurization of a disc, in plane stress, has been presented by Zhang *et al.* (1992a), Fig. 9. In this example, once again, the disc has inner and outer radii of 1 m and 1.5 m, respectively, and the inner radius is the design variable. This time, however, the disc is subjected to an external pressure rate of 5 MPa s^{-1}. It is seen that the numerically calculated sensitivity history in Zhang *et al.* (1992a) is not very accurate.

Two improvements had to be made in this work in order for the sensitivitives to become acceptably accurate for shape optimization. The first is the use of the correct formula,

$$\frac{\mathrm{d}\mathring{A}}{\mathrm{d}A} = -\frac{2}{b-a} + \frac{b}{(b-a)r}, \tag{30}$$

where r is the generic radius of the annular disc. The second is the regularization discussed in Section 2.1 of this paper. Numerical results for the sensitivity history are shown in Fig. 3. In this figure, the "semi-analytical" solution can be considered exact (see above) while "Zhang *et al.* (1992a)" refers to the use of the $O(1/r)$ singular equations in that paper, together with the correction given in eqn (30) above. Finally, the "present version" uses the regularized DBEM equations given in this paper. This version is the most accurate.

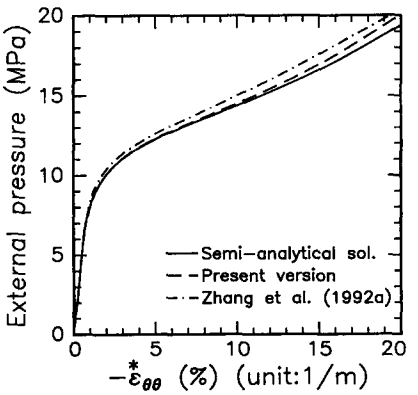

Fig. 3. External pressure as a function of $\mathring{\varepsilon}_{\theta\theta}(A)$ for a hollow disc. The simulation ends at $T = 4$ s when $\varepsilon(A) = -4.8\%$ [see also, Zhang *et al.* (1992a), Fig. 9].

4.6.2. *The optimization problem, constraints, geometry and loading history.* The problem attacked here is the elasto–viscoplastic version of the elastic optimization problem (b) above. The objective function is now ϕ_2 [eqn (22)], *evaluated at some fixed time T in the deformation history*, and the elliptical cutout is defined by eqn (28) with a fixed and $b = a\beta$ the design variable. The constraint equation used here is

$$0.5 \leqslant \beta \leqslant 1.0. \tag{31}$$

Referring to Fig. 1 and Table 1, a fixed remote loading history, for the period $0 \leqslant t \leqslant T$, is applied to the plate. The question being asked here is: *For what values of* β *(i.e. shape of the cutout) is the tangential stress around the cutout, at time T, as uniform as possible?* Except for the case $\tau_1^\infty = \tau_2^\infty$ (see Fig. 1), for which the optimal cutout shape is a circle (with $\beta = 1$), the elasto–viscoplastic solution is expected to differ from the elastic solution. This is because, for $\tau_1^\infty \neq \tau_2^\infty$, the rate of stress relaxation around the elliptical cutout will not be uniform. *Also, the optimal value of* β *is a function of the loading history and the final time* T. These issues are discussed further later in this section.

4.6.3. *Geometric sensitivitives and mesh.* The choice of mesh, especially the internal cells, is crucial for the solution of this class of problems. The best approach is to use adaptive meshing during the iterative optimization process. Work along these lines is currently in progress.

In this work, however, a fixed mesh is chosen, based on numerical experimentation of problems with known elastic and elasto–viscoplastic solutions. As mentioned earlier, the benchmark elasto–viscoplastic problem of a plate with a circular cutout and uniform remote loading has proved to be invaluable for this purpose. The mesh chosen, both boundary elements and internal cells, is shown in Fig. 4(a). In this figure, all boundary nodes are also nodes for internal cells, except on lines CD and DE where mid-boundary nodes are not connected to internal cells.

With b as the design variable, the sensitivities of geometrical quantities, used in these calculations, are as follows [see Fig. 4(b)]:

(a) Boundary
On BC, CD and DE,

$$\dot{x}_1 = \dot{x}_2 = 0, \quad \mathrm{d}\dot{S}/\mathrm{d}S = 0, \quad \mathrm{d}\dot{A}/\mathrm{d}A = 0. \tag{32}$$

On EA,

$$\dot{x}_1 = 0, \quad \dot{x}_2 = \frac{L - x_2}{L - b} \quad \text{(linear assumption)}$$

$$\frac{\mathrm{d}\dot{S}}{\mathrm{d}S} = -\frac{1}{L-b}, \quad \frac{\mathrm{d}\dot{A}}{\mathrm{d}A} = -\frac{1}{L-b}. \tag{33}$$

On AB,

$$x_1 = a\cos\theta, \quad x_2 = b\sin\theta,$$

$$\dot{x}_1 = 0, \quad \dot{x}_2 = \sin\theta = x_2/b,$$

$$\frac{\mathrm{d}\dot{S}}{\mathrm{d}S} = \frac{b^3 x_1^2}{a^4 x_2^2 + b^4 x_1^2}, \quad \frac{\mathrm{d}\dot{A}}{\mathrm{d}A} = \frac{1}{b} - \frac{x_2^2}{b^3}. \tag{34}$$

(b) Internal points
Inside the rectangle $BCDF$,

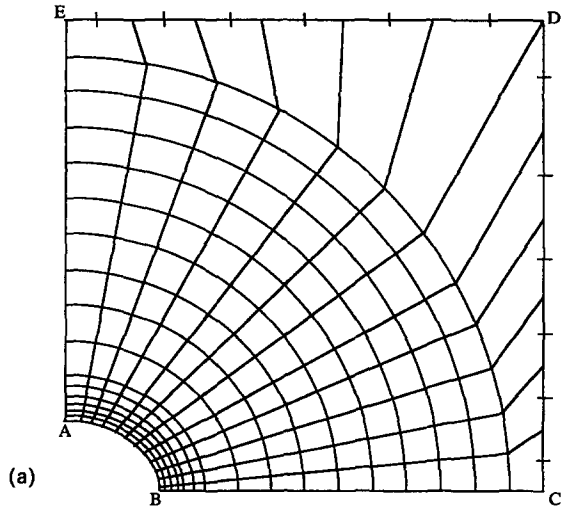

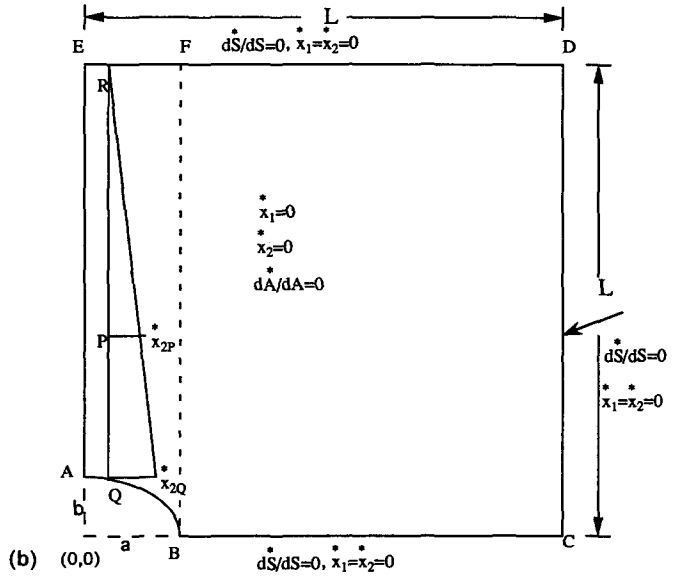

Fig. 4(a). The boundary elements and internal cells used for the elasto–viscoplastic problem. (b) Sensitivitives of geometrical quantities.

$$\dot{x}_1 = \dot{x}_2 = 0, \quad \dot{dA}/dA = 0. \tag{35}$$

Inside the region *BFEA*, using a linear assumption for the velocity $\dot{x}_2$ [see Fig. 4(b)],

$$\dot{x}_{2P} = \left(\frac{L-x_{2P}}{L-x_{2Q}}\right)\dot{x}_{2Q},$$

and

$$\frac{\dot{dA}}{dA} = -\frac{\sqrt{1-x_{1P}/a^2}}{L-b\sqrt{1-x_{1P}^2/a^2}}, \tag{36}$$

where the quantities x_{2P}, etc., are defined in Fig. 4(b). On the line *FB*,

$$\mathrm{d}\dot{A}/\mathrm{d}A = 0. \tag{37}$$

It is interesting to note that while the value of $\mathrm{d}\dot{A}/\mathrm{d}A$ inside the region *BFEA* matches the values on its boundary lines *EA* and *FB*, such is not the case on the lines *AB* and *EF*. This is expected since a separate kinematic assumption for the design velocities must be made inside the region *BFEA*. In the calculations reported next, the values of $\mathrm{d}\dot{A}/\mathrm{d}A$ on the lines *AB* and *EF* are those from eqn (36).

4.6.4. *Numerical results.* Consider, first, Fig. 1 (see, also, Table 1), with $\varepsilon = 0$, $b = a\beta$, $\tau_1^\infty = S$ and $\tau_2^\infty = 0.75\,S$. *Elastic* stress concentrations for this problem, at points *A* and *B*, can be easily shown to be (Timoshenko and Goodier, 1970)

$$\hat{\sigma}_{11}(A) = \frac{\sigma_{11}(A)}{S} = 2\frac{b}{a} + 0.25, \quad \hat{\sigma}_{22}(B) = \frac{\sigma_{22}(B)}{S} = 1.5\frac{a}{b} - 0.25. \tag{38}$$

As is well known (Banichuk, 1983), if $b/a = \tau_2^\infty/\tau_1^\infty$ (here 0.75), the load ratio

$$\frac{\sigma_{tt} \text{ on ellipse}}{S} = 1.75$$

so that the tangential stress σ_{tt} is uniform around the ellipse. This is the optimal solution for the elastic problem, as discussed before.

For the elasto–viscoplastic problem, however, the case $\tau_2^\infty/\tau_1^\infty = b/a$ does not lead to uniform relaxation of stress around the ellipse. Perhaps a useful way to see this is to define "apparent" stress concentrations at points *A* and *B* in Fig. 1. Again, for the case $\tau_1^\infty = S$ and $\tau_2^\infty = 0.75\,S$, one gets, for the elastic case,

$$\frac{\sigma_{11}(A)}{\sigma_{11}(\infty)} = 2\frac{b}{a} + 0.25, \quad \frac{\sigma_{22}(B)}{\sigma_{22}(\infty)} = 2\frac{a}{b} - 0.333. \tag{39}$$

Thus, for example, for $b/a = 0.75$, the aforementioned numbers are 1.75 and 2.333, so one might reasonably expect the tangential stress to relax faster at *B* than at *A* in the elasto–viscoplastic case. It seems reasonable to expect, therefore, that the optimal value of *b* for the elliptical cutout (with *a* fixed) should be a number other than 0.75 for the elasto–viscoplastic case. This value of *b* must be such that, starting with a nonuniform distribution of σ_{tt} around the ellipse, the tangential stress becomes uniform at a fixed (pre-chosen) time *T* into the elasto–viscoplastic deformation process. Of course, this optimal value of *b* would depend on the choice of *T* and the loading history.

With the above-mentioned preamble, the central result of this section is presented in Table 4. Here, for each value of *b*, $T = 4$ s. For the case $\beta = 0.75$, for example, the strain $\varepsilon_{11}(A, T)$ (see Fig. 1) equals 1.125%. Table 4 shows successive values of β, starting with the circle $\beta = 1$, for the shape optimization problem for the elasto–viscoplastic case. *The iterations are seen to converge, at the fifth iteration, to the value $\beta = 0.69$, with a corresponding*

Table 4. Values of β and $\phi_2(T)$ at different iterations for the elasto–viscoplastic shape optimization problem†

Number of iterations	$\beta = b/a$	ϕ_2 (MPa^2)
1	1.000	31.56600
2	0.500	14.13300
3	0.724	0.41076
4	0.697	0.03175
5	0.690	0.01052

† CPU time = 1.278 hours on an IBM 3090 supercomputer.

Table 5. Stress concentrations at A and B (Fig. 1) for different values of β†

	Elastic				Elasto–viscoplastic	
	$\sigma_{11}(A)/S(0)$		$\sigma_{22}(B)/S(0)$		$\hat{\sigma}_{11}(A, T)$	$\hat{\sigma}_{22}(B, T)$
β	Anal.	BEM	Anal.	BEM	BEM	BEM
1.000	2.250	2.380	1.250	1.224	1.619	0.943
0.500	1.250	1.206	2.750	2.874	1.097	1.627
0.724	1.698	1.714	1.822	1.885	1.324	1.250
0.697	1.644	1.653	1.902	1.972	1.298	1.284
0.690	1.630	1.636	1.924	1.998	1.290	1.294

† $\hat{\sigma}_{11}(A, T) = \sigma_{11}(A, T)/S(T)$; $\hat{\sigma}_{22}(B, T) = \sigma_{22}(B, T)/(S(T)$. Numerical results are obtained from the mesh in Fig. 4(a).

Table 6. Correlation of stress relaxation at points A and B (Fig. 1) with the "apparent" elastic strain concentrations at these points†

	"Apparent" stress concentration Elastic: Analytical		Drop in stress concentration Elasto–viscoplastic: BEM	
β	$\sigma_{11}(A)/\sigma_{11}(\infty)$	$\sigma_{22}(B)/\sigma_{22}(\infty)$	$\hat{\sigma}_{11}(A,T)/\hat{\sigma}_{11}(A,0)$	$\hat{\sigma}_{22}(B,T)/\hat{\sigma}_{22}(B,0)$
1.000	2.250	1.667	0.680	0.770
0.500	1.250	3.667	0.910	0.566
0.724	1.698	2.430	0.772	0.663
0.697	1.644	2.536	0.785	0.651
0.690	1.630	2.571	0.789	0.648
0.750	1.750	2.333	0.761	0.675

† Numerical results are obtained from the mesh in Fig. 4(a).

very low value of ϕ_2. As discussed before in this paper, the optimization algorithm used here converges when the Kuhn–Tucker optimality conditions are satisfied within an acceptable tolerance (Schittkowski, 1986).

It is useful to comment further on some of the details of this problem. Table 5 shows the stress concentrations at A and at B, for different values of β, for the elastic, as well as the elasto–viscoplastic, solution at time T. Table 6 shows the correlation of the "apparent" stress concentration at A and at B to the stress relaxation at these points in the elasto–viscoplastic case. It is seen that the point with the larger "apparent" stress concentration experiences larger relaxation of stress. The results for $\beta = 0.75$ (the elastic optimal solution) are included in Table 6. In this case, A and B have the same initial value of stress concentration, but points B, with the higher "apparent" stress concentration, experiences a larger relaxation of stress.

Figure 5 shows the tangential stress concentration around the ellipse, at time T, for various values of b. It is seen that the distribution for $b = 0.75$ is not uniform, while that for $b = 0.69$ is uniform at time T.

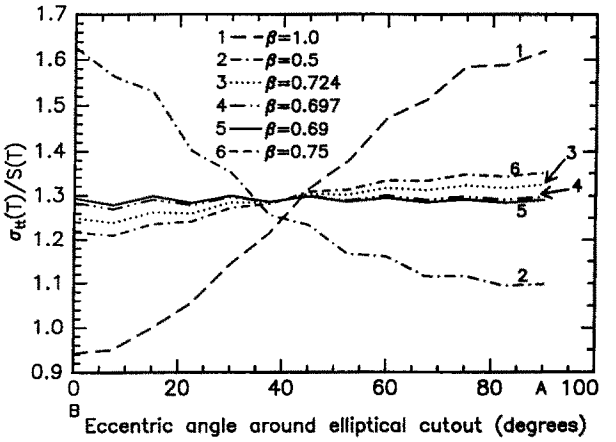

Fig. 5. Tangential stress concentration around elliptical cutout, at final time T, for different values of β.

Table 7. Stress sensitivities at A and B (Fig. 1) for different values of β†

	Elastic				Elasto–viscoplastic	
	$\mathring{\sigma}_{11}(A)/S(0)$		$\mathring{\sigma}_{22}(B)/S(0)$		$\mathring{\sigma}_{11}(A,T)/S(T)$	$\mathring{\sigma}_{22}(B,T)/S(T)$
β	Anal.	BEM	Anal.	BEM	BEM	BEM
1.000	2.0	2.540	−1.500	−1.828	1.039	−1.114
0.500	2.0	2.247	−6.000	−6.158	0.892	−2.485
0.724	2.0	2.321	−2.862	−3.181	0.901	−1.318
0.697	2.0	2.305	−3.088	−3.400	0.894	−1.398
0.690	2.0	2.301	−3.151	−3.467	0.893	−1.423
0.750	2.0	2.339	−2.667	−2.983	0.909	−1.250

† Numerical results are obtained from the mesh in Fig. 4(a). Units = m^{-1}.

Finally, something should be said about the stress sensitivities, accurate calculations of which are essential for the success of the optimization process. Differentiating equation (38) with respect to the design variable b, one gets, for the elastic problem,

$$\mathring{\sigma}_{11}(A)/S = 2/a, \quad \mathring{\sigma}_{22}(B)/S = -1.5a/b^2. \tag{40}$$

Table 7 shows the numerical and analytical values of these quantities, for the elastic problem, for various values of β, as well as the numerical values of these quantities at time T. The numerical values are calculated with the mesh shown in Fig. 4(a). A finer mesh would improve the accuracy of the results. This was demonstrated by Zhang and Mukherjee (1991), Fig. 6(b).

5. CONCLUSIONS

This paper presents, for the first time, numerical results for shape optimal design of elasto–viscoplastic continua. The approach combines shape sensitivity analysis and optimization by a sequential quadratic programming algorithm. The problem is physically nonlinear, and the sensitivities are history dependent. Great care must be exercised to numerically obtain the sensitivities, especially those of stresses, with sufficient accuracy, in order for the optimization process to be successful.

These optimization problems for physically nonlinear materials are extremely challenging from a numerical viewpoint. Adaptive meshing and vector and parallel programming are expected to be essential for the efficient solution of realistic problems with several design variables.

The first numerical results presented in this paper are extremely encouraging. Another problem of interest in the small-deformation regime, for example, is the optimal design of shapes to get the desired distribution of residual stresses in solid bodies undergoing elasto–plastic or elasto–viscoplastic deformation.

Another important goal of this ongoing research program is the optimal design of manufacturing processes—such as the design of optimal die shapes for extrusion or optimal pre-form shapes for forging. Sensitivity analysis for large-strain, large-rotation, elasto–viscoplastic problems, suitable for the design of manufacturing processes, has recently been carried out (Zhang *et al.*, 1992b). Work is now in progress in the area of optimal design of this very important class of problem.

Acknowledgements—The authors gratefully acknowledge the financial support provided by the U.S. National Science Foundation through Grant MSS 8922185 to Cornell University and The University of Arizona. All computing for this research was performed at the Cornell National Supercomputer Facility.

REFERENCES

Anand, L. (1982). Constitutive equations for the rate-dependent deformation of metals at elevated temperatures. *ASME J. Engng Mater. Tech.* **104**, 12–17.

Banichuk, N. V. (1983). *Problems and Methods of Optimal Structural Design*. Plenum Press, New York.
Cardoso, J. B. and Arora, J. S. (1988). Variational methods for design sensitivity analysis in nonlinear structural mechanics. *AIAA Jl* **26,** 595–602.
Choi, K. K. and Santos, J. L. T. (1987). Design sensitivity analysis of nonlinear structural systems; part I: Theory. *Int. J. Num. Meth. Engng* **24,** 2039–2055.
Cruse, T. A. and Vanburen, W. (1971). Three-dimensional elastic stress analysis of a fracture specimen with an edge crack. *Int. J. Fract. Mech.* **7,** 1–15.
Golub, G. H. and Van Loan, C. F. (1989). *Matrix Computations* (2nd Edn). The Johns Hopkins University Press, Baltimore and London.
Haftka, R. T., Gurdal, Z. and Kamat, M. P. (1990). *Elements of Structural Optimization* (2nd edn). Kluwer, Dordrecht, The Netherlands.
Haug, E. J., Choi, K. K. and Komkov, V. (1986). *Design Sensitivity Analysis of Structural Systems*. Academic Press, New York.
Lekhnitski, S. G. (1968). *Anisotropic Plates* (2nd Edn) (translated by S. W. Tsai and T. Cheron). Gordon and Breach, New York.
Mukherjee, S. (1982). *Boundary Element Methods in Creep and Fracture*. Elsevier Applied Science, London.
Mukherjee, S. and Chandra, A. (1987). Nonlinear solid mechanics. In *Boundary Element Methods in Mechanics* (Edited by D. Beskos), pp. 285–331. North-Holland, Amsterdam.
Mukherjee, S. and Chandra, A. (1989). A boundary element formulation for design sensitivitives in materially nonlinear problems. *Acta Mech.* **78,** 243–253.
Mukherjee, S. and Chandra, A. (1991). A boundary element formulation for design sensitivities in problems involving both geometric and material nonlinearities. *Math. and Comp. Modelling* **15,** 245–255.
Nagarajan, A. and Mukherjee, S. (1993). A mapping method for numerical evaluation of two-dimensional integrals with $1/r$ singularity. *Comput. Mech.* **12,** 19–26.
Park, J. S. and Choi, K. K. (1990). Design sensitivity analysis of critical load factor for nonlinear structural systems. *Comput. Struct.* **36,** 823–838.
Sadegh, A. M. (1988). On the Green's functions and boundary integral formulation of elastic planes with cutouts. *Mech. Struct. Mach.* **16,** 293–311.
Santos, J. L. T. and Choi, K. K. (1988). Sizing design sensitivity analysis of nonlinear structural systems; part II: Numerical method. *Int. J. Num. Meth. Engng* **26,** 2097–2114.
Schittkowski, K. (1986). NLPQL: A FORTRAN subroutine solving constrained nonlinear programming problems. *Ann. Oper. Res.* **5,** 485–500.
Sladek, V. and Sladek, J. (1986). Improved computation of stresses using the boundary element method. *Appl. Math. Modelling* **10,** 249–255.
Timoshenko, S. P. and Goodier, J. N. (1970). *Theory of Elasticity* (3rd Edn). McGraw-Hill, New York.
Tortorelli, D. A. (1988). Design sensitivity analysis for nonlinear dynamic thermoelastic systems. Ph.D. thesis, University of Illinois at Urbana–Champaign.
Tortorelli, D. A. (1990). Sensitivity analysis for nonlinear constrained elastostatic systems. In *Symposium on Design Sensitivity Analysis and Shape Optimization Using Numerical Methods* (Edited by S. Saigal and S. Mukherjee), pp. 115–126. ASME, New York.
Tsay, J. J. and Arora, J. S. (1990). Nonlinear structural design sensitivity analysis for path dependent problems; part I: General theory. *Comput. Meth. Appl. Mech. Engng* **81,** 183–208.
Tsay, J. J., Cardoso, J. E. B. and Arora, J. S. (1990). Nonlinear structural design sensitivity analysis for path dependent problems; part 2: Analytical examples. *Comput. Meth. Appl. Mech. Engng* **81,** 209–228.
Wu, C. C. and Arora, J. S. (1987). Design sensitivity analysis and optimization of nonlinear structure response using incremental procedures. *AIAA Jl* **25,** 1118–1125.
Zhang, Q. and Mukherjee, S. (1991). Design sensitivity coefficients for linear elastic bodies with zones and corners by the derivative boundary element methods. *Int. J. Solids Structures* **27,** 983–998.
Zhang, Q., Mukherjee, S. and Chandra, A. (1992a). Design sensitivity coefficients for elasto–viscoplastic problems by boundary element methods. *Int. J. Num. Meth. Engng* **34,** 947–966.
Zhang, Q., Mukherjee, S. and Chandra, A. (1992b). Shape design sensitivity analysis for geometrically and materially nonlinear problems by the boundary element method. *Int. J. Solids Structures* **29,** 2503–2525.
Zhao, Z. (1991). *Shape Design Sensitivity Analysis and Optimization Using the Boundary Element Method*. Springer, New York and Berlin.